



**GDE2 Promotes Neurogenesis by
Glycosylphosphatidylinositol-Anchor Cleavage of RECK**
Sungjin Park *et al.*
Science **339**, 324 (2013);
DOI: 10.1126/science.1231921

This copy is for your personal, non-commercial use only.

If you wish to distribute this article to others, you can order high-quality copies for your colleagues, clients, or customers by [clicking here](#).

Permission to republish or repurpose articles or portions of articles can be obtained by following the guidelines [here](#).

The following resources related to this article are available online at www.sciencemag.org (this information is current as of January 17, 2013):

Updated information and services, including high-resolution figures, can be found in the online version of this article at:

<http://www.sciencemag.org/content/339/6117/324.full.html>

Supporting Online Material can be found at:

<http://www.sciencemag.org/content/suppl/2013/01/16/339.6117.324.DC1.html>

This article **cites 30 articles**, 9 of which can be accessed free:

<http://www.sciencemag.org/content/339/6117/324.full.html#ref-list-1>

This article appears in the following **subject collections**:

Cell Biology

http://www.sciencemag.org/cgi/collection/cell_biol

and the maiden name of the mother matched exactly to the grandfathers' surnames, substantially increasing the confidence of the recovery. Coriell also lists the ages (23) during sample collection for these two pedigrees, which agreed with the age differences of all tested cases with the identified family members. Using genealogical Web sites, we traced the patrilineal lineage that connects each identified genome through the MRCA to the record originator in the genetic genealogy database (Fig. 3). This analysis revealed that two to seven meiosis events link the CEU genome to the record source. Finally, we calculated that the probability of finding random families in the Utah population with these exact demographic characteristics is less than 1 in 10^5 to 5×10^9 (13). In total, surname inference breached the privacy of nearly 50 individuals from these three pedigrees.

This study shows that data release, even of a few markers, from one person can spread through deep genealogical ties and lead to the identification of another person who might have no acquaintance with the person who released his genetic data. The propagation of information through shared male lines amplifies the range of identification, allowing ~135,000 records to potentially target several million U.S. males. Another feature of this identification technique is that it entirely relies on free, publicly available resources. It can be completed end-to-end with only computational tools and an Internet connection. The compatibility of our technique with public record search engines makes it much easier to continue identifying other data sets in the same pedigree, including female genomes, once one male target is identified. We envision that the risk of surname inference will grow in the future. Genetic genealogy enthusiasts add thousands of records to these databases every month. In addition, the advent of third-generation sequencing platforms with longer reads will enable even higher coverage of Y-STR markers, further strengthening the ability to link haplotypes and surnames.

Similar to other genetic privacy issues (24–30), preventing surname inference from public whole-genome data sets might be quite challenging. Masking Y-STR markers could limit the effectiveness of the method presented in this study, but this approach is not sustainable (13). Our analysis suggests that Y-STR haplotypes can be imputed back from single-nucleotide polymorphisms (SNPs) on the Y chromosome (Y-SNPs) when a large reference set of male genomes will be available (fig. S6). In addition, community efforts, such as the Y Chromosome Genome Comparison, have already started exploring the association between Y-SNPs and surnames (table S1) and might allow bypassing Y-STR masking. We also posit that restricting genetic genealogy information is not practical, as some of the data are already scattered in multiple end-user Web sites and genealogy mailing lists.

Existing policy tools, such as controlled-access databases with data use agreements, may mediate the exposure of genomic information to surname inference. However, in our view, the appropriate

response to genetic privacy challenges is not for the public to stop donating samples or for data sharing to stop. These would be devastating reactions that could substantially hamper scientific progress. Rather, we believe that establishing clear policies for data sharing, educating participants about the benefits and risks of genetic studies (31), and the legislation of proper usage of genetic information (32) are pivotal ingredients to support the genomic endeavor.

References and Notes

1. B. Sykes, C. Irven, *Am. J. Hum. Genet.* **66**, 1417 (2000).
2. T. E. King, S. J. Ballereau, K. E. Schürer, M. A. Jobling, *Curr. Biol.* **16**, 384 (2006).
3. B. McEvoy, D. G. Bradley, *Hum. Genet.* **119**, 212 (2006).
4. T. E. King, M. A. Jobling, *Mol. Biol. Evol.* **26**, 1093 (2009).
5. T. E. King, M. A. Jobling, *Trends Genet.* **25**, 351 (2009).
6. R. Lehmann-Haupt, "Are sperm donors really anonymous anymore?" *Slate*, 1 March 2010.
7. G. Naik, "Family secrets: An adopted man's 26-year quest for his father," *Wall Street Journal*, 2 May 2009.
8. R. Stein, "Found on the Web, with DNA: A boy's father," *Washington Post*, 13 November 2005.
9. A. Motluk, *New Sci.* **188**, 6 (3 November 2005).
10. J. E. Lunshof, R. Chadwick, D. B. Vorhaus, G. M. Church, *Nat. Rev. Genet.* **9**, 406 (2008).
11. J. Gitschier, *Am. J. Hum. Genet.* **84**, 251 (2009).
12. L. L. Rodriguez, L. D. Brooks, J. H. Greenberg, E. D. Green, *Science* **339**, 275 (2013).
13. See supplementary materials on Science Online.
14. *Federal Register: 45 CFR 164.514(b-c)* (2002).
15. M. Gymrek, D. Golan, S. Rosset, Y. Erlich, *Genome Res.* **22**, 1154 (2012).
16. N. Leat, L. Ehrenreich, M. Benjeddou, K. Cloete, S. Davison, *Forensic Sci. Int.* **168**, 154 (2007).
17. S. K. Lim, Y. Xue, E. J. Parkin, C. Tyler-Smith, *Int. J. Legal Med.* **121**, 124 (2007).
18. S. Levy et al., *PLoS Biol.* **5**, e254 (2007).
19. Full details of this analysis were provided to the reviewers. However, they are not presented here to

respect the privacy of these families. Further inquiries can be made to the corresponding author.

20. http://hapmap.ncbi.nlm.nih.gov/downloads/elsi/CEPH_Reconsent_Form.pdf.
21. The 1000 Genomes Project Consortium, *Nature* **467**, 1061 (2010).
22. S. M. Prescott, J. M. Lalouel, M. Leppert, *Annu. Rev. Genomics Hum. Genet.* **9**, 347 (2008).
23. Based on the results of this study, the NIH removed the ages from Coriell to a secure location (12).
24. Z. Lin, A. B. Owen, R. B. Altman, *Science* **305**, 183 (2004).
25. F. R. Bieber, C. H. Brenner, D. Lazer, *Science* **312**, 1315 (2006).
26. N. Homer et al., *PLoS Genet.* **4**, e1000167 (2008).
27. K. B. Jacobs et al., *Nat. Genet.* **41**, 1253 (2009).
28. H. K. Im, E. R. Gamazon, D. L. Nicolae, N. J. Cox, *Am. J. Hum. Genet.* **90**, 591 (2012).
29. D. W. Craig et al., *Nat. Rev. Genet.* **12**, 730 (2011).
30. E. E. Schadt, S. Woo, K. Hao, *Nat. Genet.* **44**, 603 (2012).
31. A. L. McGuire, R. A. Gibbs, *Science* **312**, 370 (2006).
32. Presidential Commission for the Study of Bioethical Issues, Privacy and Progress in Whole Genome Sequencing. Privacy and Progress in Whole Genome Sequencing (2012).

Acknowledgments: We thank FamilyTreeDNA and SMGF for technical assistance. We also thank D. Esposito, A. Goren, G. Fink, D. Page, W. Kramer, and R. Ronen for useful discussions. Y.E. is an Andria and Paul Heafy Family Fellow. This publication was supported by a gift from Jim and Cathy Stone (Y.E.), the National Defense Science and Engineering Graduate Fellowship (M.G.), and the Edmond J. Safra Center for Bioinformatics at Tel-Aviv University (D.G. and E.H.).

Supplementary Materials

www.sciencemag.org/cgi/content/full/339/6117/321/DC1
Supplementary Text
Figs. S1 to S6
Tables S1 to S7
References

31 August 2012; accepted 3 December 2012
10.1126/science.1229566

GDE2 Promotes Neurogenesis by Glycosylphosphatidylinositol-Anchored Cleavage of RECK

Sungjin Park,^{1*} Changhee Lee,^{1*} Priyanka Sabharwal,¹ Mei Zhang,¹ Caren L. Freel Meyers,² Shanthini Sockanathan^{1†}

The six-transmembrane protein glycerophosphodiester phosphodiesterase 2 (GDE2) induces spinal motor neuron differentiation by inhibiting Notch signaling in adjacent motor neuron progenitors. GDE2 function requires activity of its extracellular domain that shares homology with glycerophosphodiester phosphodiesterases (GDPDs). GDPDs metabolize glycerophosphodiester to glycerol-3-phosphate and corresponding alcohols, but whether GDE2 inhibits Notch signaling by this mechanism is unclear. Here, we show that GDE2, unlike classical GDPDs, cleaves glycosylphosphatidylinositol (GPI) anchors. GDE2 GDPD activity inactivates the Notch activator RECK (reversion-inducing cysteine-rich protein with kazal motifs) by releasing it from the membrane through GPI-anchor cleavage. RECK release disinhibits ADAM (a disintegrin and metalloproteinase) protease-dependent shedding of the Notch ligand Delta-like 1 (Dll1), leading to Notch inactivation. This study identifies a previously unrecognized mechanism to initiate neurogenesis that involves GDE2-mediated surface cleavage of GPI-anchored targets to inhibit Dll1-Notch signaling.

The transition from cellular proliferation to differentiation is tightly controlled so as to ensure appropriate numbers of distinct

cell types are formed and to prevent the depletion or uncontrolled proliferation of progenitor cells. Glycerophosphodiester phosphodiesterase 2

(GDE2) is necessary and sufficient to induce differentiation of spinal motor neuron (MN) subtypes. GDE2 acts non-cell-autonomously by inhibiting Notch signaling in neighboring Oligodendrocyte transcription factor 2 ($Olig2^+$) MN progenitors using extracellular glycerophosphodiester phosphodiesterase (GDPD) domain activity (1–4). Because Notch is activated by ligands Delta-like (Dll) and Jagged (Jag) expressed in adjacent cells, we tested whether GDE2 might target Dll1 and Jag1 function (3, 5). Jag1 and Dll1 are expressed in nonoverlapping domains within the ventral spinal cord, and genetic ablation of either ligand causes domain-specific precocious neuronal differentiation (fig. S1A) (5–7). Spinal cords of mice lacking GDE2 ($Gde2^{-/-}$) showed a specific loss of MNs and V0 interneurons, no changes in the total number of V1 interneurons or V2 interneurons, but an increase in the ratio of V2a:V2b interneurons (Fig. 1, A to I) (3). These domain-specific deficits correspond to regions of Dll1 expression and function, suggesting that GDE2 specifically targets Dll1 but not Jag1 activity (fig. S1A).

Dll1 is inactivated through cleavage and release of its extracellular domain (ECD) by the ADAM (a disintegrin and metalloproteinase) metalloproteinase family (5). To determine whether GDE2 GDPD activity promotes Dll1 shedding, we coelectroporated plasmids expressing GDE2 and C-terminal Flag-tagged Dll1 (Dll1-Flag) into chick spinal cords and analyzed Dll1 processing by means of protein immunoblotting. Overexpression of Dll1-Flag generated full-length Dll1 and a processed 30-kD C-terminal fragment (CTF) (Fig. 1J). Overexpression of GDE2 and Dll1-Flag induced accumulation of a C-terminal 42-kD Dll1 product (Dll1-42) that was not generated by coexpression of the two-pass transmembrane GDPD protein GDE1 (4, 8) or by catalytically inactive GDE2 GDPD mutants (GDE2.APML) (Fig. 1J) (3). A corresponding N-terminal Dll1 ECD fragment was detected after overexpressing a double-tagged version of Dll1 (Myc-Dll1-Flag) (fig. S2). Fluorescence-activated cell sorting (FACS) analysis of Dll1 expression showed decreased Dll1 surface expression in MNs when GDE2 was overexpressed in chick spinal cords and a corresponding increase of endogenous Dll1 surface expression in GFP⁺ MNs purified from $HB9:GFP;Gde2^{-/-}$ animals (fig. S3) (9). Consistent with the Dll1-specific function of GDE2, no changes in Jag1 expression (Jag1FL) or processing (Jag1CTF) were detected in spinal cords overexpressing GDE2 or in spinal cords of $Gde2^{-/-}$ animals (Fig. 1, J and K). These data indicate that GDE2 GDPD activity stimulates Dll1 processing and decreases

the availability of cell-surface Dll1 in vivo. In addition to removing surface Dll1 for Notch receptor activation, the released Dll1 ECD is reported to inhibit Notch signaling by a dominant-negative activity (5); thus, Dll1 should function cooperatively with GDE2 to induce MN differentiation. Indeed, overexpression of GDE2 with Dll1 in chick spinal cords enhanced the ability of GDE2 to induce premature differentiation of ventricular zone (VZ) progenitors into $Isl2^+$ MNs (Fig. 1, L to N).

GDE2 did not induce Dll1-42 accumulation when coexpressed with Dll1-Flag in heterologous human embryonic kidney (HEK) 293T cells; thus, GDE2-dependent processing of Dll1 is likely indirect (fig. S1B). Overexpression of ADAM10 and Dll1-Flag in chick spinal cords induced formation of Dll1-42 and decreased surface Dll1, suggesting that Dll1-42 may be generated through ADAM metalloprotease activity (figs. S3B and S4). Further, ADAM10 that was overexpressed in chick spinal cords effectively cleaved Dll1 Δ clv, which lacks a reported ADAM10 cleavage site mapped in vitro (10), suggesting that Dll1-42 may be generated by ADAM proteolytic activity through a separate cleavage site that is preferentially used in vivo (fig. S4). Thus, GDE2 GDPD activity appears to stimulate ADAM-dependent processing of Dll1 to Dll1-42, inducing MN differentiation.

The GPI-anchored protein, reversion-inducing cysteine-rich protein with kazal motifs (RECK), activates Notch signaling in cortical progenitors by directly inhibiting ADAM10-dependent Dll1 processing (11, 12). RECK mRNA is enriched in VZ cells and overlaps with GDE2 expression in newly differentiating MNs during neurogenesis (fig. S5, A and B). Depletion of RECK in spinal cords by two different short hairpin RNAs (shRNAs) (fig. S5, C and D) lowered Notch signaling as assayed by reduced expression of downstream Notch target genes *Hes5* and *Blbp* (5) and the induction of premature MN differentiation in the VZ (Fig. 2, A to L). Moreover, loss of RECK specifically induced accumulation of Dll1-42 in spinal cords but did not alter Jag1 expression and processing to Jag1CTF (Fig. 2M). These phenotypes are similar to those caused by GDE2 overexpression and indicate that GDE2 GDPD activity may promote Dll1 shedding by inactivating RECK (1–3).

To determine how GDE2 GDPD activity might inactivate RECK, we tested whether GDE2 exhibits classical GDPD phospholipase-D (PLD) catalysis in a coupled spectrophotometric assay of GDPD function (Fig. 3, A and B) (13). Membrane fractions of HEK293T cells transfected with control GDE1 showed GDPD activity when incubated with glycerophosphoserine (GPSerine), or a cyclic glycerol-1,2-phosphate intermediate (cyG[1,2]P) that is not substrate-specific and formed by GDPD enzymes during their predicted two-step catalytic mechanism (Fig. 3, A and B) (14). However, GDE2 showed no GDPD activity in either case (Fig. 3B). The GDPD domains of the six-transmembrane GDEs (GDE2, GDE3, and

GDE6) are homologous to the catalytic X domain of phosphatidylinositol phospholipase C (PI-PLC). GDE3, unlike GDE1, hydrolyzes GPIPinositol through a PLC-type cleavage mechanism (15, 16). Because exogenous bacterial PI-PLCs cleave and release GPI-linked proteins from membranes, we tested whether GDE2 GDPD activity inactivates RECK through GPI-anchor cleavage. We overexpressed GDE2 and RECK in HEK293T cells and assayed the culture medium for cleaved RECK ECD by means of protein immunoblotting. GDE2 and RECK coexpression released RECK into the medium, as does treatment with PI-PLC, whereas medium prepared from cells that were transfected with vector alone, GDE1, or catalytically inactive GDE2.APML contained little RECK (Fig. 3, C and E). Repeated Triton X-114 extraction of medium from cells overexpressing GDE2 and RECK yielded RECK in hydrophilic fractions, ruling out potential medium contamination by membrane-bound RECK (Fig. 3D) (17). Further, sequential expression of RECK and GDE2 released RECK into the medium (fig. S6), suggesting that GDE2 acts on surface GPI-anchored RECK and does not promote aberrant RECK discharge through disruption of RECK synthesis, modification, or transport. Consistent with inactivation of RECK by GDE2 through cleavage of its GPI-anchor, endogenous RECK processing examined by Triton X-114 partitioning of cortical extracts showed reduced RECK release in $Gde2^{-/-}$ animals compared with that of wild-type (WT) littermates (fig. S7).

To date, two vertebrate GPI-anchor cleaving enzymes have been identified that use phospholipase-type cleavage mechanisms, GPI-PLD, and the vertebrate homolog of *Drosophila* Notum (18, 19). Notum failed to release RECK into the medium of transfected HEK293T cells, whereas GPI-PLD led to effective RECK cleavage (fig. S8A). Analysis of surface biotinylated RECK in transfected HEK293T cells showed that GDE2 activity releases biotinylated RECK from the surface membrane into the medium; in contrast, GPI-PLD did not, suggesting that GPI-PLD cleavage of RECK is intracellular and occurs within the endoplasmic reticulum or Golgi (Fig. 3F). Taken together, these observations indicate that GDE2-mediated release of RECK occurs on the cell surface and is independent from the function of known vertebrate GPI-anchor-cleaving enzymes.

To define the mechanism of RECK release by GDE2, we radiolabeled transfected HEK293T cells and confirmed that the RECK ECD released into the medium by GDE2 expression contained components of the GPI-anchor such as [³H] inositol or [³H] ethanolamine, whereas a secreted version of RECK ECD (sRECK) that lacked the GPI-anchor was poorly labeled under identical conditions (Fig. 3G and fig. S8B) (20). Moreover, cells overexpressing RECK in which the GPI-anchor was replaced with the transmembrane domain from the non-GPI-anchored CD2 protein failed to produce RECK in the medium in the presence of GDE2 (fig. S9, A and B) (21, 22). These observations indicate that RECK release by

¹Solomon Snyder Department of Neuroscience, School of Medicine, Johns Hopkins University, PCTB1004, 725 N Wolfe Street, Baltimore, MD 21205, USA. ²Department of Pharmacology and Molecular Sciences, School of Medicine, Johns Hopkins University, WBSB 301A, 725 N Wolfe Street, Baltimore, MD 21205, USA.

*These authors contributed equally to this work.

†To whom correspondence should be addressed. E-mail: ssockan1@jhmi.edu

GDE2 involves specific cleavage within the GPI-anchor—a concept supported by the ability of GDE2 to cleave other unrelated GPI-anchored proteins, such as the glypicans GPC2 and GPC4

(fig. S10). PLD cleavage of the GPI-anchor would result in loss of a phosphate group from the phosphatidylinositol domain of released RECK when compared with PLC cleavage mechanisms (Fig.

3G). Comparison of radiolabeled [³²P] incorporation between RECK ECD generated by GDE2 or GPI-PLD expression normalized to [³H] inositol levels showed that RECK released by GDE2

Fig. 1. Stimulation of Dll1 shedding by GDE2. (A to H) Coronal sections of embryonic day 13 (E13.5) mouse spinal cords. Arrows mark V2b interneurons (red). (I) Graph quantifying interneuron numbers in WT and *Gde2*^{-/-} mutants; mean ± SEM, *n* = 4 embryos, two-tailed *t* test: V0, **P* = 0.0016; V1, *P* = 0.4778; V2a, **P* = 0.0028; V2b, **P* = 0.0088. (J) Western blots of extracts of chick spinal cords electroporated with Dll1-Flag plasmid; in the top blot, the open arrow indicates 30-kD Dll1 C-terminal fragment, and the solid arrow indicates C-terminal 42-kD Dll1 product (Dll1-42). In the top middle blot, the solid arrow (GDE2) indicates endogenous glycosylated GDE2, and the bottom bands are hypoglycosylated GDE2. (K) Western blot of Jag1 processing (FL, full length; CTF, C-terminal fragment) and quantification of Jag1 CTF/FL ratios from E12.5 embryonic spinal cord extracts. (L to N) Close-up of electroporated chick spinal cords (right) shows increased *Isl2*⁺ MNs (red) when Dll1 is coelectroporated with GDE2. Arrows indicate midline. Scale bar, 20 μm.

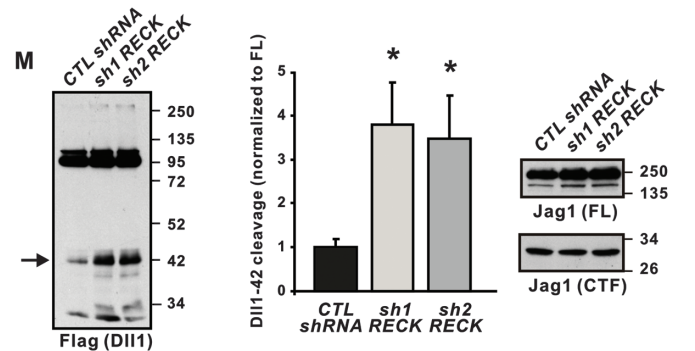
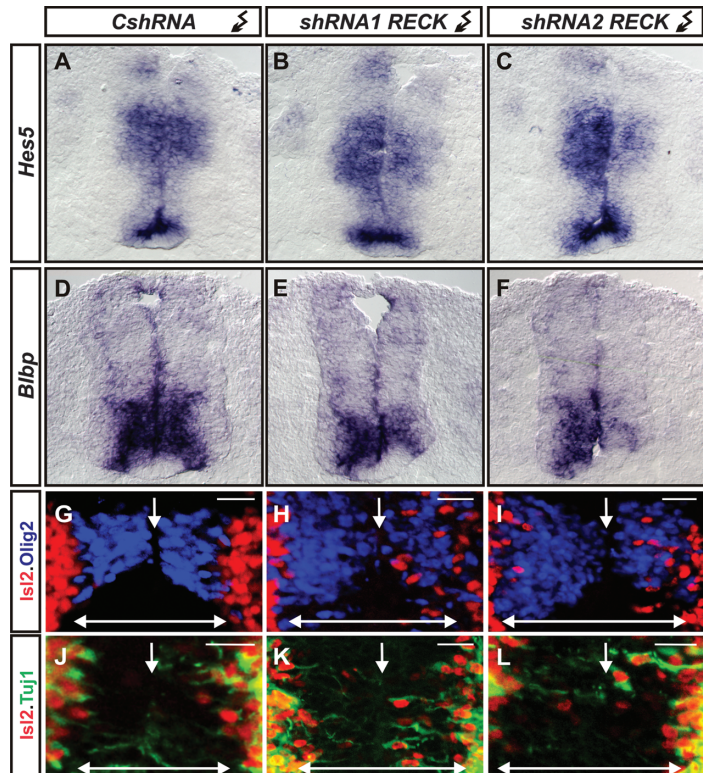
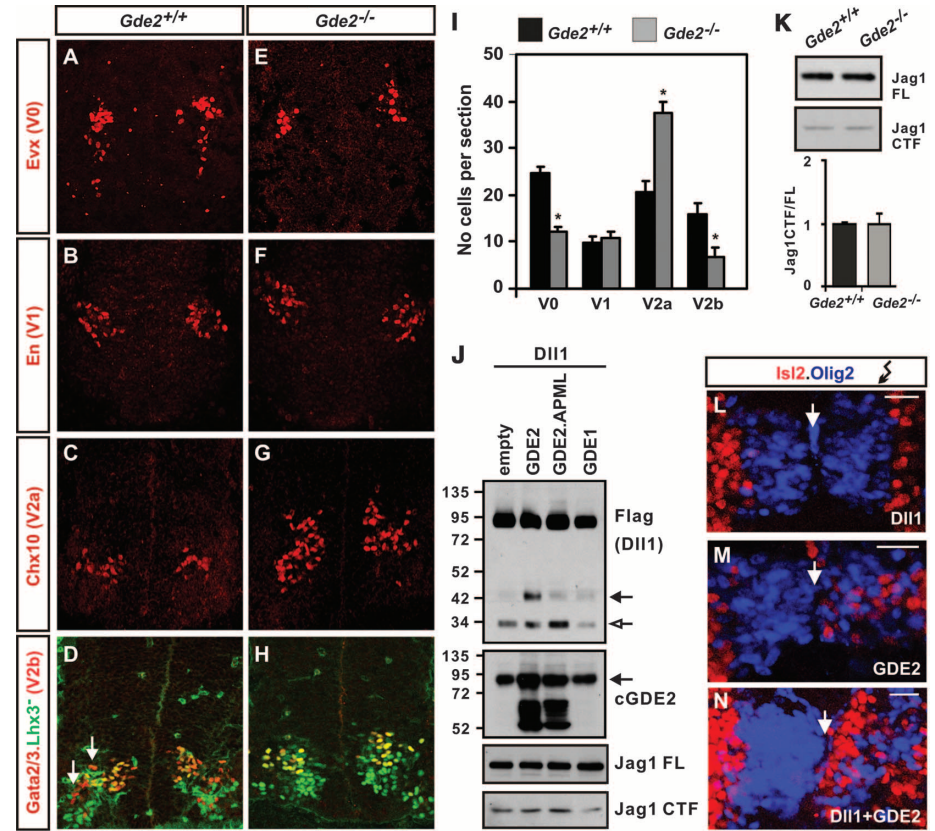


Fig. 2. Effects of RECK ablation. (A to F) Notch target gene mRNAs are reduced in HH stages 19/20 chick spinal cords electroporated with *RECK* shRNAs but not control shRNAs (*CshRNAs*). (G to L) *Olig2* expression (blue) demarcates VZ of chick spinal cords electroporated (right) with control and *RECK* shRNAs, showing *Isl2*⁺ MNs (red) that express neuronal Tuj1 (green) when *RECK* is knocked down. Arrows indicate midline; double-headed arrows indicate VZ. Scale bar, 20 μm. (M) Western blots of chick spinal cords electroporated with Dll1-Flag plasmid and *RECK* shRNAs show *RECK* knockdown stimulates Dll1-42 production (arrow), but Jag1 expression and processing is unchanged. Shown is a graph quantifying Dll1-42 cleavage from Western blots; mean ± SEM. Two-tailed *t* test, *n* = 4 embryos; *sh1RECK* **P* = 0.0066; *sh2RECK* **P* = 0.0175.

Fig. 3. GDE2 cleaves RECK within the GPI-anchor. (A) Schematic of two-step GDPD catalysis. (B) Graph quantifying in vitro GDPD assay in transfected HEK293T cells using glycerophosphoserine (GPserine) and synthetic cyclic glycerol[1,2] phosphate intermediate. v, empty vector. (C to E) Western blots of transfected HEK293T cell lysates (lys) and medium (med). (C) RECK is detected in the medium when catalytically active GDE2 is present. (D) After sequential Triton X-114 extraction cleaved, RECK is observed in the Detergent (DT)-free hydrophilic phase, whereas Dll1, which is not cleaved by GDE2, is retained in the DT-rich hydrophobic phase of the lysate. (E) RECK ECD is generated by GDE2 or PI-PLC activities. (F) Western blot of lysates (lys) and medium (med) of HEK293T cells transfected with RECK and C-terminal Flag-tagged GDE2 or GPI-PLD. Surface RECK is labeled by biotin. GDE2 but not GPI-PLD releases surface-biotinylated RECK into the medium (arrow). Both GDE2 and GPI-PLD are visualized by antibodies to Flag, but only GDE2 is labeled by biotin, indicating that GDE2 is localized to the cell surface. PI-PLC was added to intact cells and serves as a positive control. (G) Schematic of GPI-anchor (top) and graph quantifying amount of radiolabel incorporated into RECK or sRECK when GDE2 or PI-PLC is present (bottom). Mean \pm SEM; $n = 4$ to 12 samples.

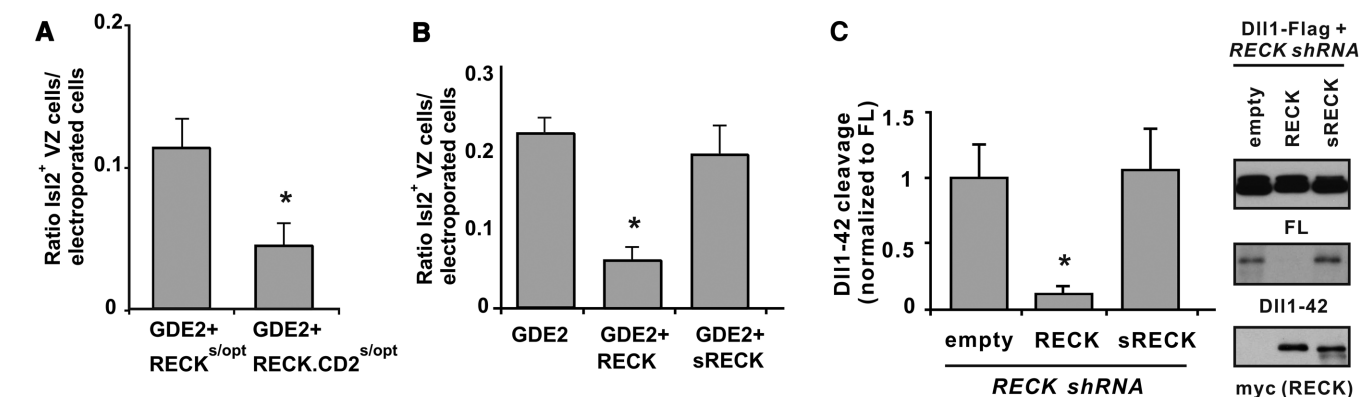
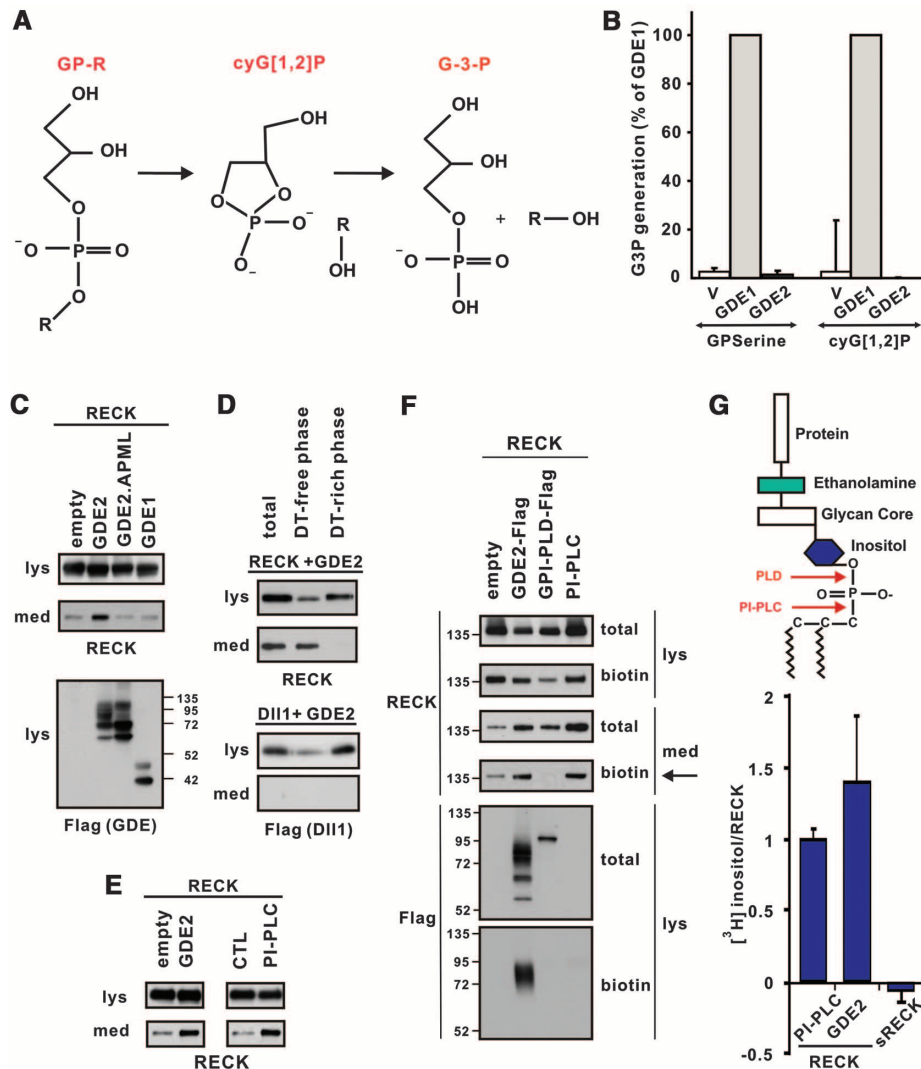


Fig. 4. GDE2 inactivates RECK through GPI-anchor cleavage. (A and B) Graphs quantifying ratio of ectopic IsI2⁺ VZ MNs normalized to the number of transfected GDE2 cells. Mean \pm SEM, two-tailed *t* test. (A) Suboptimal levels of plasmids expressing RECK^{s/opt} or RECK-CD2^{s/opt} were coelectroporated with GDE2. RECK-CD2 was more effective than was RECK in suppressing GDE2-dependent MN generation. **P* = 0.0306; $n = 5$ embryos. (B) Plasmids expressing RECK or sRECK were coelectroporated with GDE2; RECK effectively

suppressed GDE2 function, but sRECK did not (**P* = 5.59×10^{-5} ; $n = 8$ to 10 embryos) as compared with GDE2. (C) Western blot of extracts of chick spinal cords electroporated with Dll1-Flag and RECK shRNA targeting 3' untranslated region to detect full-length (FL) and processed Dll1-42. The phenotype is rescued by exogenous plasmids expressing WT RECK open reading frame but not sRECK. Densitometric quantification of Dll1-42, mean \pm SEM, $n = 4$ embryos. Two-tailed *t* test, **P* = 0.013 compared with empty.

contained higher ratios of [32 P]:[3 H] inositol than when cleaved by GPI-PLD (table S1). This observation suggests that GDE2 release of RECK does not use a similar mechanism to GPI-PLD. Bacterial PI-PLC cleavage of GPI linkages creates a distinct stable 1,2 cyclic inositol phosphate ring (cyIno[1,2]P), which is recognized by antibodies to cross-reacting determinant (CRD) (23, 24). RECK ECD generated from GDE2 overexpression did not cross-react with antibodies to CRD (fig. S8C), suggesting that GDE2 cleavage of GPI-anchors is different to that of bacterial PI-PLC; however, this observation is consistent with reports that mammalian PLC enzymes have different kinetics to bacterial PI-PLCs and fail to generate stable cyclic intermediates (25).

If GDE2 inactivates RECK to induce MN differentiation, then overexpression of RECK might overcome GDE2 inhibition and suppress GDE2-dependent induction of premature MN generation in the VZ. We used Cre-lox techniques to generate mosaic expression of GDE2 in *Olig2*⁺ MN progenitors. This caused neighboring cells to differentiate into *Isl2*⁺ MNs (3, 26). WT GPI-anchored RECK overexpressed with GDE2 effectively suppressed GDE2-dependent premature MN differentiation (Fig. 4B and fig. S9, E and F). Overexpressed RECK-CD2 more effectively suppressed GDE2 induction of MN differentiation than did equivalent amounts of GPI-anchored RECK (Fig. 4A and fig. S9, C and D), further indicating that GDE2 inactivates RECK to induce MN differentiation through cleavage of the GPI-anchor.

RECK ECD generated after GPI-anchor cleavage should be inactive and fail to maintain *Olig2*⁺ MN progenitors through Notch activation. However, soluble versions of RECK that lack the GPI-anchor are active in other systems, suggesting that the activity of cleaved RECK is context-dependent (11). Using similar Cre-lox approaches, we compared the effects of WT RECK and sRECK to inhibit GDE2-dependent MN generation in electroporated chick spinal cords. Overexpression of WT RECK with GDE2 suppressed GDE2-dependent premature differentiation of MNs (Fig. 4B and fig. S9F); in contrast, sRECK failed to suppress GDE2 activity (Fig. 4B and fig. S9G). WT RECK was sufficient to prevent increased *Dll1* shedding resulting from ablation of endogenous RECK by shRNAs, whereas sRECK had no effect (Fig. 4C). These observations suggest that RECK ECD fails to inhibit *Dll1* shedding and imply that GDE2 GDPD-dependent cleavage of RECK clears active RECK from the membrane.

Our data suggest a model in which GDE2 promotes MN differentiation by inactivating surface-bound RECK through GPI-anchor cleavage, thus allowing ADAM protein function (fig. S11). GDE2 cleaves GPI-anchored proteins at the cell surface in multiple *in vitro* and *in vivo* contexts that are independent of known GPI-anchor-cleaving enzymes. These observations support direct modes of cleavage, an activity shared by its family members GDE3 and GDE6 (fig. S10) (4); nevertheless, it remains possible that their function could in-

volve stimulation of unidentified cleaving enzymes. GPI-anchored proteins are key regulators of signaling pathways that control diverse biological processes in the developing and adult organism (27, 28). Understanding how these pathways are regulated through GPI-anchor cleavage in normal and diseased states might be gained by further analysis of six-transmembrane GDE GDPD protein expression, transport, and activity.

References and Notes

- M. Rao, S. Sockanathan, *Science* **309**, 2212 (2005).
- Y. Yan, P. Sabharwal, M. Rao, S. Sockanathan, *Cell* **138**, 1209 (2009).
- P. Sabharwal, C. Lee, S. Park, M. Rao, S. Sockanathan, *Neuron* **71**, 1058 (2011).
- N. Yanaka, *Biosci. Biotechnol. Biochem.* **71**, 1811 (2007).
- B. D'Souza, L. Meloty-Kapella, G. Weinmaster, *Curr. Top. Dev. Biol.* **92**, 73 (2010).
- C. E. Lindsell, J. Boulter, G. diSibio, A. Gossler, G. Weinmaster, *Mol. Cell. Neurosci.* **8**, 14 (1996).
- U. Marklund *et al.*, *Development* **137**, 437 (2010).
- B. Zheng, C. P. Berrie, D. Corda, M. G. Farquhar, *Proc. Natl. Acad. Sci. U.S.A.* **100**, 1745 (2003).
- H. Wichterle, I. Lieberam, J. A. Porter, T. M. Jessell, *Cell* **110**, 385 (2002).
- E. Six *et al.*, *Proc. Natl. Acad. Sci. U.S.A.* **100**, 7638 (2003).
- T. Muraguchi *et al.*, *Nat. Neurosci.* **10**, 838 (2007).
- J. S. Rhee, L. M. Coussens, *Trends Cell Biol.* **12**, 209 (2002).
- N. Ohshima *et al.*, *J. Bacteriol.* **190**, 1219 (2008).
- L. Shi, J. F. Liu, X. M. An, D. C. Liang, *Proteins* **72**, 280 (2008).
- D. Corda *et al.*, *J. Biol. Chem.* **284**, 24848 (2009).
- M. J. Rebecchi, S. N. Pentylala, *Physiol. Rev.* **80**, 1291 (2000).
- T. L. Doering, P. T. Englund, G. W. Hart, *Curr. Protoc. Protein Sci.* Chap. 12, Unit 12.5 (2001).

- H. Tsujioka, Y. Misumi, N. Takami, Y. Ikehara, *Biochem. Biophys. Res. Commun.* **251**, 737 (1998).
- A. Traister, W. Shi, J. Filmus, *Biochem. J.* **410**, 503 (2008).
- M. G. Paulick, C. R. Bertozzi, *Biochemistry* **47**, 6991 (2008).
- A. Gallet, L. Staccini-Lavenant, P. P. Théron, *Dev. Cell* **14**, 712 (2008).
- D. Yan, Y. Wu, Y. Feng, S. C. Lin, X. Lin, *Dev. Cell* **17**, 470 (2009).
- J. D. Bangs, D. Hereld, J. L. Krakow, G. W. Hart, P. T. Englund, *Proc. Natl. Acad. Sci. U.S.A.* **82**, 3207 (1985).
- S. E. Zamze, M. A. Ferguson, R. Collins, R. A. Dwek, T. W. Rademacher, *Eur. J. Biochem.* **176**, 527 (1988).
- D. W. Heinz, L. O. Essen, R. L. Williams, *J. Mol. Biol.* **275**, 635 (1998).
- B. Zhuang, Y. S. Su, S. Sockanathan, *Neuron* **61**, 359 (2009).
- D. Yan, X. Lin, *Cold Spring Harb. Perspect. Biol.* **1**, a002493 (2009).
- A. Fico, F. Maina, R. Dono, *Cell. Mol. Life Sci.* **68**, 923 (2011).

Acknowledgements: We thank P. Englund, M. Goulding, T. M. Jessell, and B. Novitch for antibodies; J. Filmus for Notum plasmids; the Flow Cytometry and Cell Sorting Core Facility, Johns Hopkins Bloomberg School of Public Health; C. Cave III, A. L. Kolodkin, P. F. Worley, and Y. Yan for comments on the manuscript; and lab members for discussions. This work was funded by National Institute of Neurological Disorders and Stroke RO1NS046336.

Supplementary Materials

www.sciencemag.org/cgi/content/full/339/6117/324/DC1
Materials and Methods
Figs. S1 to S11
Table S1
References (29–34)

23 October 2012; accepted 19 November 2012
10.1126/science.1231921

Interstitial Dendritic Cell Guidance by Haptotactic Chemokine Gradients

Michele Weber,¹ Robert Hauschild,¹ Jan Schwarz,¹ Christine Mousson,¹ Ingrid de Vries,¹ Daniel F. Legler,² Sanjiv A. Luther,³ Tobias Bollenbach,¹ Michael Sixt^{1*}

Directional guidance of cells via gradients of chemokines is considered crucial for embryonic development, cancer dissemination, and immune responses. Nevertheless, the concept still lacks direct experimental confirmation *in vivo*. Here, we identify endogenous gradients of the chemokine CCL21 within mouse skin and show that they guide dendritic cells toward lymphatic vessels. Quantitative imaging reveals depots of CCL21 within lymphatic endothelial cells and steeply decaying gradients within the perilymphatic interstitium. These gradients match the migratory patterns of the dendritic cells, which directionally approach vessels from a distance of up to 90-micrometers. Interstitial CCL21 is immobilized to heparan sulfates, and its experimental delocalization or swamping the endogenous gradients abolishes directed migration. These findings functionally establish the concept of haptotaxis, directed migration along immobilized gradients, in tissues.

Several guidance cues operate in vertebrates, with the most prominent group being chemokines. *In vitro*, many chemokines induce directional cell migration when offered as gradients. However, the best established *in vivo* example of chemokine function does not rely on gradients: During extravasation from the blood stream, chemokines immobilized on the luminal surface of blood vessels (1–3) trigger the local arrest of leukocytes, which precedes their exit

into the tissue (4). Less is known about how chemokines act beyond the endothelium (5), and, especially within lymphatic organs, chemokines seem to rather cause random motility than directional responses (5). The sparse body of existing evidence for directional guidance is largely inferred from the migratory trajectories of cells without information on actual chemokine distribution (6–8). Only two studies visualized chemokine gradients in parenchymal organs (9, 10),